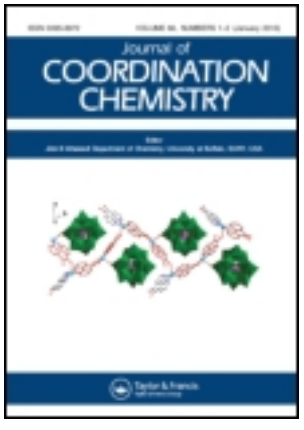

Journal of Coordination Chemistry
Publication details, including instructions for authors and subscription information:
http://www.tandfonline.com/loi/gcoo20

Role of the metal sites of a heterobimetallic trinuclear complex on DNA binding and cleavage activities

Anangamohan Panja [a]

[a] Postgraduate Department of Chemistry , Panskura Banamali College , Panskura RS , India

Published online: 03 Jun 2013.

To cite this article: Anangamohan Panja (2013) Role of the metal sites of a heterobimetallic trinuclear complex on DNA binding and cleavage activities, Journal of Coordination Chemistry, 66:12, 2178-2190, DOI: 10.1080/00958972.2013.801466

To link to this article: http://dx.doi.org/10.1080/00958972.2013.801466

Journal of Coordination Chemistry, 2013
Vol. 66, No. 12, 2178–2190, http://dx.doi.org/10.1080/00958972.2013.801466

Role of the metal sites of a heterobimetallic trinuclear complex on DNA binding and cleavage activities

ANANGAMOHAN PANJA*

Postgraduate Department of Chemistry, Panskura Banamali College, Panskura RS, India

(*Received 20 December 2012; in final form 12 March 2013*)

Reaction of $(PPh_4)[Fe(pzcq)(CN)_3]$ with cobalt(II) nitrate afforded a heterobimetallic trinuclear complex $[Fe(pzcq)(CN)_3]_2[Co(H_2O)_2(MeOH)_2]\cdot 2H_2O$ (**1**), where Hpzcq is 8-(pyrazine-2-carboxamido)quinoline. The structural data show that crystallographically equivalent [(pzcq)Fe $(CN)_3]^-$ units are monodentate ligands through one of the three cyanides to cobalt(II) in **1**. Interaction of **1** with *calf thymus* DNA was investigated through UV–vis and fluorescence spectroscopic methods and viscosity measurements. Complex **1** preferably binds with CT-DNA in the groove region and promotes DNA cleavage in the presence of H_2O_2 as an activating agent. The DNA cleavage proceeds through an oxidative pathway possibly through a diffusible hydroxyl radical mechanism. The nuclease activity of **1** can be explained by cooperation of two different metal sites, the aromatic rings of pzcq in iron(III) are responsible for binding with DNA, while diffusible hydroxyl radical generated *in situ* by the reaction of cobalt(II) center with hydrogen peroxide is likely to be involved for cleavage of DNA.

Keywords: Heterobimetallic trinuclear complex; DNA binding; Nuclease activity; Role of metal sites

1. Introduction

Development of artificial chemical nucleases has grown in the last few decades [1–3]. Successful chemical nucleases have extensive applications as DNA sensors, antitumour drugs, and artificial restriction enzymes [4, 5]. Among the different therapeutic strategies to destroy cancer cells through DNA damage, the use of small water soluble metal complexes, capable of oxidative or hydrolytic DNA cleavage as anticancer drugs, is a demanding topic in bioinorganic chemistry, biotechnology, and molecular biology [6–8]. Platinum-based drugs, for example cisplatin and carboplatin, are the most widely used antitumor metallodrugs for the treatment of certain human cancers with remarkable success but severe toxic side effects, including nephrotoxicity and increased drug resistivity, prevent their potential efficiency [9, 10]. Ruthenium(II) and biorelevant copper(II) compounds are promising alternatives to platinum-based drugs because of their improved anticancer activity and lower toxicity compared to platinum compounds [11–15]. To design effective chemotherapeutic agents and better anticancer drugs, it is essential to explore the interaction of metal complexes with DNA by intercalation, groove binding, and the

*Email: ampanja@yahoo.co.in

external electrostatic force. These studies are also important to understand the toxicity of metallo drugs [16].

Biorelevant cobalt and iron complexes have gained increasing attention for their applicability [17, 18]. Previous reports describe that hexamine cobalt complexes induce DNA condensation and can be used to probe RNA hairpins [19, 20]. [Co(tfa)(happ)] functions as a specific probe for DNA bulges due its ability to cleave DNA specifically [21]. The DNA binding and photocleavage activity of certain cobalt(II) complexes have been reported [22, 23]. Iron bleomycins (Fe-BLMs), potent members of the bleomycin family of antitumor glycopeptide antibiotics, are used in chemotherapy because of their ability to engage in direct double strand cleavage by the delivery of two oxidizing equivalents to the DNA helix [24, 25]. This oxidative cleavage mechanism limits the scope to realize the full therapeutic potential of such complexes as they require activation by either light or an oxidant, and so the antitumor activity of these complexes has not been well explored [26–28]. However, redox-active agents that damage DNA *in vitro* might show apoptotic activities in living systems by inducing oxidative stress and/or damage of DNA [29, 30]. Thus, redox-active cobalt and iron complexes, which may cleave DNA by generating Reactive Oxygen Species (ROS) *in vitro*, are potential anticancer drugs [31, 32].

We have recently reported both hydrolytic and oxidative DNA cleavage agents [33, 34]; a photoactive dinuclear zinc(II) complex with an azobenzene linker showed remarkable hydrolytic DNA cleavage activity [33]. The *trans* form of the complex was inactive while its *cis* congener exhibited efficient DNA cleavage, and two closely located Zn(II) centers in the *cis* form were cooperatively involved in cleavage. I envisioned that incorporation of two different coordination sites may cooperatively engage in DNA binding and cleavage. Herein, I report the synthesis and crystal structure of a heterobimetallic trinuclear complex, $[Fe(pzcq)(CN)_3]_2[Co(H_2O)_2(MeOH)_2]\cdot 2H_2O$ (**1**), and the role of metal sites in DNA binding and cleavage activities.

2. Experimental

2.1. *Materials and physical measurements*

$(PPh_4)[Fe(pzcq)(CN)_3]$ was synthesized according to the literature method [35]. Pyrazine-2-carboxylic acid, iron(III) chloride hexahydrate, cobalt(II) nitrate hexahydrate, 8-aminoquinoline, and tris(hydroxymethyl)aminomethane (Tris) were purchased from Aldrich and Alfa Aesar. *Calf thymus* DNA (CT-DNA) and ethidium bromide (EB) were purchased from Sigma. All other chemicals and solvents were of reagent or analytical grade and used as received.

Elemental analyses for C, H, and N were performed by the Pregl–Dumas technique on a Thermo Fischer Flash EA1112 analyzer, while metal contents were determined using a Perkin–Elmer 200 atomic absorption spectrometer. FTIR spectra of the complexes were recorded from 400 to 4000 cm^{-1} on a Nicolet 750 Magna-IR spectrometer using KBr pellets. Absorption spectra were measured using a Shimadzu UV-2450 spectrophotometer with a 1 cm path length quartz cell. Fluorescence experiments were performed with a Hitachi F-4500 spectrofluorometer. Conductivity measurements were made with a Systronics (model 304) direct reading conductivity meter.

2.2. *Syntheses of $[Fe(pzcq)(CN)_3]_2[Co(H_2O)_2(MeOH)_2]\cdot 2H_2O$ (1)*

To a 20 mL methanolic solution of $(PPh_4)[Fe(pzcq)(CN)_3]$ (0.10 mM) was added an aqueous solution (3 mL) of $Co(NO_3)_2\cdot 6H_2O$ (0.05 mM) with stirring. The combined dark red solution was allowed to stand at room temperature. Dark-red crystals suitable for X-ray diffraction were obtained from the solution after several days. Yield: 0.040 g, 42%. Anal. Calcd for $C_{36}H_{34}CoFe_2N_{14}O_8$: C, 44.98%; H, 3.56%; N, 20.39%; Co, 6.13%; Fe, 11.61%. Found: C, 45.28%; H, 3.52%; N, 19.99%; Co, 6.55%; Fe, 11.96%. IR (KBr, cm^{-1}): 3412 br ($\nu_{NH,\ OH}$); 1668 m ($\nu_{C=O}$). 2116, 2143 m ($\nu_{C\equiv N}$). Molar conductance: $10\ \Omega^{-1}\ cm^2\ mol^{-1}$.

2.3. *X-ray crystallography*

Intensity data for **1** were collected at low temperature with a Nonius Kappa CCD diffractometer using graphite-monochromated Mo Kα radiation ($\lambda = 0.71073$ Å). Cell refinement, indexing, and scaling of the datasets were performed using DENZO-SMN and SCALEPACK [36]. The structure was solved by direct methods using SHELXS and refined by the full-matrix least-square based on F^2 using SHELXL [37] with all the reflections. Thermal parameters for nonhydrogen atoms were refined anisotropically. All hydrogens bound to carbon were placed in calculated positions using a riding model, while those attached to oxygen were located in the difference Fourier map and refined using fixed isotropic thermal parameters based on their respective parent. All calculations were performed using the WinGX System, Ver. 1.70.01 [38]. The crystal parameters and basic information

Table 1. Crystal data and structure refinements for **1**.

Empirical formula	$C_{36}H_{34}CoFe_2N_{14}O_8$
Formula weight	961.40
Temperature (K)	150(2)
Wavelength (Å)	0.71073
Crystal system	Monoclinic
Space group	C2/c
Unit cell dimensions	
a (Å)	20.2316(7)
b (Å)	14.3925(4)
c (Å)	15.0670(5)
β (°)	113.147(1)
Volume (Å^3)	4034.1(2)
Z	4
D_{calc} (g cm^{-3})	1.583
Absorption coefficient (mm^{-1})	1.186
F(0 0 0)	1964
Crystal size (mm)	0.16 × 0.08 × 0.06
θ range for data collection (°)	2.89–27.44
Reflections collected	8960
Independent reflections/R_{int}	4579/0.0344
Observed reflections [$I > 2\sigma(I)$]	3381
Data/restraints/parameters	4579/4/292
Goodness-of-fit on F^2	1.050
Final *R* indices [$I > 2\sigma(I)$]	$R_1 = 0.0416$, $wR_2 = 0.1044$
R indices (all data)	$R_1 = 0.0659$, $wR_2 = 0.1141$
Largest diff. peak/hole (e Å^{-3})	1.284/−0.544

Table 2. Selected bond lengths (Å) and angles (°) for **1**.

Co1–O2	2.124(2)	Fe1–N4	1.952(2)
Co1–O3	2.086(2)	Fe1–C15	1.963(3)
Co1–N6	2.093(3)	Fe1–C16	1.949(3)
Fe1–N1	1.966(2)	Fe1–C17	1.947(3)
Fe1–N2	1.886(2)		
N5–C15–Fe1	177.1(3)	N6–C16–Fe1	178.4(3)
N7–C17–Fe1	179.5(3)	C16–N6–Co1	176.8(3)

relating to data collections and structure refinements for **1** are summarized in table 1 and bond lengths and angles in table 2.

2.4. *DNA binding and cleavage studies*

Using electronic absorption spectral method, the intrinsic binding of **1** to CT-DNA was studied in 2% DMF/20 mM phosphate buffer at pH 7.5. The ratio of UV absorbance at 260 and 280 nm of CT-DNA solution was 1.9, indicating that DNA was sufficiently free of protein [39]. The concentration of CT-DNA was determined from its absorption intensity at 260 nm with a molar extinction coefficient of 6600 $M^{-1}\,cm^{-1}$ [40]. Complex **1** at fixed concentration was titrated with increasing amounts of CT-DNA and the changes in the absorption spectra were recorded after incubation for 5 min.

Fluorescence spectroscopy was used to measure the relative binding affinity of a complex to CT-DNA. For this purpose, EB-bound CT-DNA (2.5×10^{-5} M) in 2% DMF/20 mM phosphate buffer (pH 7.5) was excited at 510 nm and the fluorescence intensities at 602 nm of EB-bound CT-DNA were recorded at each incremental addition of **1** after incubation for 5 min.

Viscosity experiments were carried out using an Ostwald viscometer at room temperature. Flow time was measured with a digital stopwatch and each sample was measured three times, and an average flow time was calculated. Data were presented as $(\eta/\eta_0)^{1/3}$ versus [complex]/[DNA], where η and η_0 are the specific viscosities of CT DNA solution in the presence and absence of **1**, respectively. The viscosity values were calculated from the observed flow time of CT-DNA containing solutions (t), duly corrected for that of buffer alone (t_0), $\eta = (t - t_0)/t_0$ [41].

Plasmid DNA (pUC19) was extracted and purified according to the literature method [33]. DNA cleavage activity of **1** was determined by monitoring the conversion of supercoiled plasmid DNA (Form I) to nicked circular DNA (Form II) using agarose gel electrophoresis. The cleavage reaction was initiated by mixing plasmid DNA (0.005 μg/μL) with **1** in 2% DMF/20 mM phosphate buffer (pH 7.5) and was quenched by the addition of loading buffer containing equal volumes of a 10 × DNA loading buffer (Takara-bromophenol blue) and a 10 mM aqueous solution of ethylenediaminetetraacetic acid (EDTA). After electrophoresis, the resulting gel was transferred to an EB solution (1 μg/1 μL) and stained. The bands of the supercoiled and nicked circular DNA forms were visualized and the extent of cleavage of the SC DNA was quantified by measuring intensities of the bands using the Gel Documentation System (Bio Rad). A correction factor of 1.3 was utilized to account for the decreased ability of EB to intercalate into Form I DNA compared to Form II [42]. Cleavage mechanistic investigation of pUC19 DNA was carried out in the presence of standard radical scavengers and reaction inhibitors.

3. Results and discussion

3.1. *Synthesis and structure of 1*

Treatment of $(PPh_4)[Fe(pzcq)(CN)_3]$ to an aqueous methanol solution of cobalt(II) nitrate afforded heterobimetallic trinuclear **1**. The product is independent of the stoichiometry of the reactants which may be due to the favorable self-assembly neutralization process occurring in the reaction. Purity of the bulk sample was checked by elemental analysis and by atomic absorption spectroscopy. Molar conductivity reveals that **1** is not an electrolytic. The infrared spectra of **1** have cyano stretches characteristics of those observed for related complexes [35, 43–45]. As typical for polynuclear complexes containing cyano bridges, the infrared spectrum for **1** exhibits two ν_{CN} stretches (2143 and 2116 cm^{-1}), suggesting that both bridging and terminal cyanides are present. Higher and lower energy bands are ascribed as bridging and terminal cyanides, respectively.

3.2. *Description of the crystal structures*

Complex **1** crystallizes in the monoclinic C2/c space group, where the asymmetric unit corresponds to half of the complex molecule along with lattice water. In the crystal structure, the central Co resides on a twofold axis parallel to the crystallographic *b* axis, and a C2 rotation about this axis transposes the coordinates of half of the atoms in the molecule to the other half. The perspective view of **1** along with selected atom numbering scheme is depicted in figure 1. Crystallographically equivalent iron(III) centers are coordinated by three pzcq nitrogens and three cyanide carbons meridionally. The Fe–C(cyano) [1.946(3)–1.961(3) Å] and Fe–N(pzcq) bond lengths [1.886(2)–1.967(2) Å) are in agreement with those observed in other low-spin iron(III) complexes [35,43–45]. The Fe–C≡N angles for both terminal [177.1(3)° and 179.5(3)°] and bridging [178.3(3)°] cyanide are very close to linear. In this trinuclear cluster, the $[(pzcq)Fe(CN)_3]^-$ units are monodentate ligands through a cyanide towards *cis* positions of the central $[Co(H_2O)_2(CH_3OH)_2]^{2+}$ core, resulting in a bent structure.

The cobalt is six-coordinate in a squashed octahedral geometry, comprised of two waters, two methanols, and two cyanides from two tricyanoferrates(III). The Co–O(water), Co–O(methanol), and Co–N(cyano) distances are 2.089(2), 2.124(2), and 2.093(3) Å,

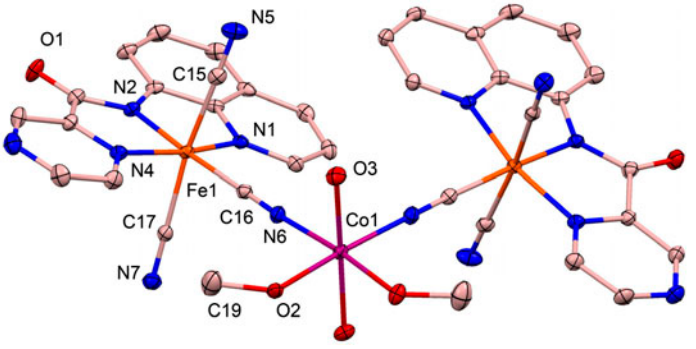

Figure 1. Crystal structure of **1** showing the atom numbering scheme. Ellipsoids are drawn with 30% probability. Hydrogens and solvent molecules are omitted for clarity.

Table 3. Geometry of important hydrogen bonds (Å, °) for **1**.

D–H···A	D–H	H···A	D···A	∠D–H···A
O2–H2A···N7a	0.74(4)	2.02(4)	2.735(4)	164(4)
O3–H3A···O1b	0.94(3)	1.92(4)	2.839(3)	165(3)
O3–H3B···O4	0.97(3)	1.71(4)	2.671(4)	174(4)
O4–H4A···N5c	1.07(3)	1.81(3)	2.871(4)	177(4)
O4–H4B···N5d	0.92(5)	2.16(5)	3.048(4)	164(5)

Symmetry codes: a = x, 2 − y, 1/2 + z; b = 1/2 + x, 1/2 + y, z; c = 1 − x, y, 1/2 − z; d = −1/2 + x, 3/2 − y, −1/2 + z.

respectively, comparable to those found for high-spin cobalt(II) complexes [46]. The Co–N≡C bond angle [176.8(3)°] is close to linear. Both coordinated and noncoordinated waters together with amide oxygen, coordinated methanol, and terminal cyanides are involved in strong hydrogen bonding to stabilize crystal packing (table 3). Symmetry-related lattice waters and coordinated cyanide nitrogens from the two adjacent molecules form supramolecular aggregates through hydrogen-bonded square-like grids as shown in figure S1. Moderately, strong face to face (3.682 Å) π–π stacking interactions are observed between aromatic rings of adjacent molecules. The intramolecular Fe···Co and Fe···Fe separations are 5.19 and 7.29 Å, respectively, and the shortest intermolecular Fe···Fe, Co···Fe, and Co···Co distances are 8.52, 6.84, and 7.54 Å, respectively.

3.3. *DNA binding studies*

DNA binding is a critical step for DNA cleavage in most cases. Thus, the binding ability of the complex with DNA is characterized by UV–vis spectroscopy. Small molecules that π stack between the two DNA base pairs are DNA intercalators, showing larger bathochromic shift and hypochromism of the spectral bands [47]. The extent of hypochromism is commonly consistent with the strength of intercalation. Complex **1** exhibits intense absorption in the UV region, attributed to intraligand π–π* transition of coordinated pzcq. The binding of **1** to CT-DNA was determined by monitoring the change in the absorption intensity of the complex with the increasing concentration of CT-DNA in 2% DMF/20 mM phosphate buffer at pH 7.5. Absorption spectra of **1** in the absence and presence of CT-DNA at different concentrations are given in figure 2. Spectral titrations show that upon addition of increasing amounts of CT-DNA to the complex only moderate hypochromism without any significant band shift was observed. The intrinsic binding constant (K_b) was determined by the following equations [48]:

$$(\varepsilon_a - \varepsilon_f)/(\varepsilon_b - \varepsilon_f) = (b - (b^2 - 2K_b^2 C_t[\mathrm{DNA}]/s)^{1/2})/(2K_b C_t);$$

$$b = 1 + K_b C_t + K_b[\mathrm{DNA}]/2s$$

where ε_a, ε_f, and ε_b are extinction coefficients at a given DNA concentration, the complex free in solution and the complex fully bound to DNA, respectively. C_t is the total metal complex concentration, [DNA] is the DNA concentration in nucleotides, and s is the binding site size in base pairs. The intrinsic binding constant (K_b) of the complex was

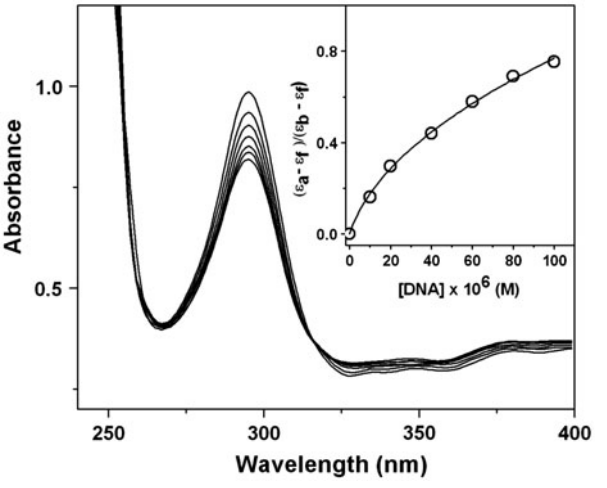

Figure 2. Absorption spectral titration upon incremental addition of CT-DNA (0–1.0×10^{-4} M) to **1** (2.0×10^{-5} M) in 2% DMF/20 mM phosphate buffer (pH 7.5) at room temperature. Inset: plot of $(\varepsilon_a - \varepsilon_f)/(\varepsilon_b - \varepsilon\varepsilon_f)$ *vs.* [DNA].

$(1.26 \pm 0.05) \times 10^4\,M^{-1}$. The absence of any extended aromatic moiety together with the smaller K_b of $(1.26 \pm 0.05) \times 10^4\,M^{-1}$ compared to those reported for typical intercalators certainly indicate that the complex does not bind to DNA through intercalation [49]. As neutral species, the possibility of electrostatic binding of **1** to CT-DNA is excluded. The K_b value is comparable to those found for small metal complexes that interact with DNA in groove regions, clearly suggesting that the association of **1** with CT-DNA is likely to be via groove binding.

Competitive binding essays were employed to further clarify the interaction of **1** with DNA, as no luminescence was observed for the complex at room temperature in aqueous solution or in the presence of CT-DNA. Although the emission intensity of EB in buffer medium is quenched by solvent molecules, it is enhanced when strongly stacked between adjacent DNA base pairs [50]. Intercalation of a molecule to EB-bound DNA decreases the emission intensity by the release of EB from DNA, and extent of reduction of the emission intensity is used to measure its binding propensity to DNA [51]. Titration of **1** with pretreated EB-bound DNA shows that the fluorescence intensity was not effectively quenched (figure 3). The quenching constant of the complex was evaluated by the classical Stern–Volmer equation [52],

$$I_0/I = 1 + K_{SV} \times r$$

where I_0 and I are the fluorescence intensities in absence and presence of the quencher, respectively. K_{SV} is the linear Stern–Volmer quenching constant, and r is the concentration ratio of the quencher to DNA. The quenching constant K_{SV} was 0.07 for **1**, indicative of weaker affinity of **1** to CT-DNA than EB. The relative binding constant (K_{app}) of the complex was evaluated from the equation [53]:

$$K_{EB} \times [EB]_{1/2} = K_{app} \times [complex]_{1/2}$$

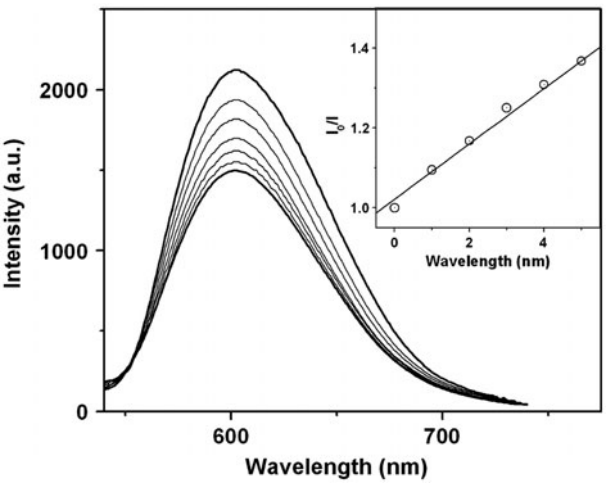

Figure 3. Fluorescence emission spectral changes ($\lambda_{ex} = 510$ nm) by addition of increasing amount of **1** (0–12.5×10^{-5} M) to EB-bound CT-DNA (2.5×10^{-5} M, 1 : 1). Inset: plot of I_0/I *vs.* [complex **1**]/[DNA].

where $[EB]_{1/2}$ (2.5×10^{-5} M) and $[complex]_{1/2}$ are the concentration of the EB and complex, respectively, at 50% reduction of the fluorescence intensity. $[Complex]_{1/2}$ was obtained from extrapolation of the plot of I_0/I versus [complex]/[DNA] as 1.25×10^{-3} M (figure 3, inset) for **1**. K_{EB} represents the binding constant between EB and CT-DNA ($K_{EB} = 1.4 \times 10^6\,M^{-1}$) [49]. The K_{app} for the complex to EB bound CT-DNA was $2.8 \times 10^4\,M^{-1}$ for **1**. This is consistent with the above trend in DNA binding affinities obtained from the absorption spectroscopy. These results support the hypothesis that **1** does not bind through intercalation, since the obtained binding constants of the complex to DNA is much smaller than that of EB [49].

Because of its sensitivity to the change of length of DNA, viscosity measurement is an effective means to study the binding mode of complex to DNA, especially in the absence of crystallographic structure data [54]. A significant increase in the viscosity of DNA on the addition of a complex indicates the intercalative mode of binding to DNA. In contrast, complex that binds in the DNA grooves by partial and/or nonclassical intercalation causing less pronounced (positive or negative) or no change in DNA solution viscosity [55, 56]. Viscosity measurements were carried out on CT-DNA by varying the concentration of **1**. The plot of $(\eta/\eta_0)^{1/3}$ versus [complex]/[DNA] (figure 4) reveals that the viscosity of DNA is almost unchanged upon addition of the complex. These results also support that **1** does not intercalate with DNA, and possibly groove binding is operative. This may be explained by partial insertion of the complex between DNA base pairs, leading to a slight increase in the separation of base pairs and, thus an increase in overall DNA contour length.

From the preceding results, it can be concluded that binding the complex to DNA through intercalation and electrostatic binding does not occur for **1**. Groove binding is operative through interaction of the aromatic rings of pzcq ligands with the base pairs of DNA. Both iron(III) centers in **1** are equivalent and connected with pzcq, and thus the binding to DNA is mainly regulated by iron(III) sites with no contribution from the cobalt (II) center.

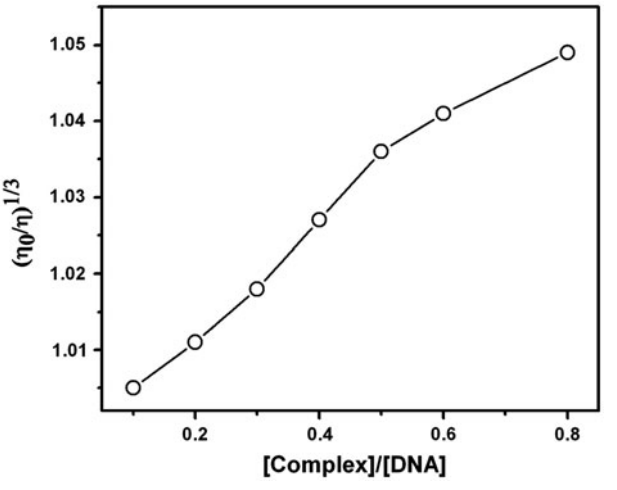

Figure 4. Changes of the relative viscosity of CT-DNA (100 μM) upon addition of increasing amounts of **1** at room temperature in 2% DMF/20 mM phosphate buffer (pH 7.5).

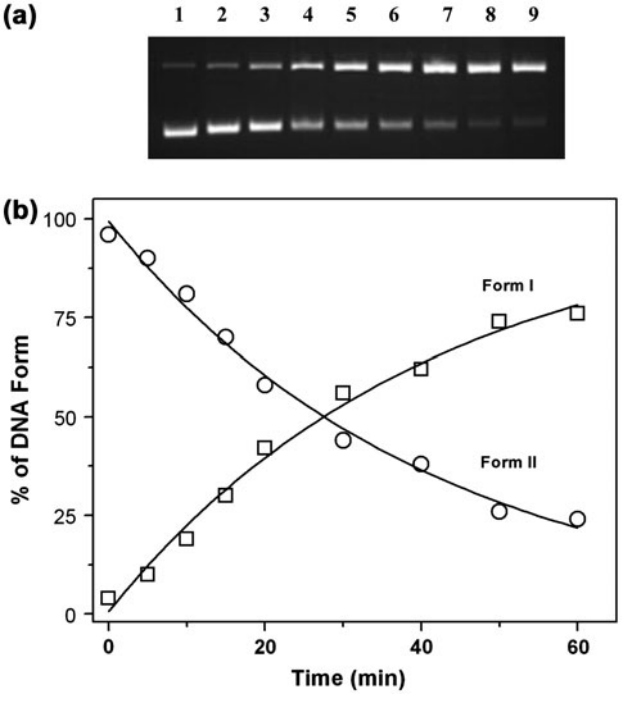

Figure 5. Time course of DNA cleavage promoted by **1** (60 μM) in the presence of H_2O_2 (100 mM) in 2% DMF/20 mM phosphate buffer (pH 7.5) at 37 °C. (A) Agarose gel electrophoresis patterns of pUC19 DNA (0.005 μg/μL) are shown at various reaction times: lanes 1–9: reaction times of 0, 5, 10, 15, 20, 30, 40, 50, and 60 min, respectively. (B) Plots of percentages of supercoiled (Form I) and nicked-circular (Form II) DNA *vs.* reaction time.

3.4. *DNA cleavage activity*

DNA cleavage of **1** was examined by monitoring the conversion of supercoiled pUC19 DNA (Form I) to nicked circular (Form II) using agarose gel electrophoresis to separate the cleavage products. Complex **1** shows efficient DNA cleavage in the presence of hydrogen peroxide as an activating agent. In control experiments, the complex or H_2O_2 alone do not exhibit significant DNA cleavage activity. The cleavage reactions were studied using different complex concentrations and incubation times. The gel electrophoretic separations of plasmid pUC19 DNA induced by increasing concentrations of **1** is shown in figure S2. Cleavage efficiency of the complex gradually increases with the increase in concentration of the complex, indicating that DNA cleavage activity of **1** is clearly dependent on its concentration. Time resolved gel electrophoresis pattern of pUC19 DNA cleavage by **1** is shown in figure 5. With increase in reaction time, the amount of Form II increased with concominent disappearance of Form I. The results demonstrate that **1** can effectively cleave DNA in the presence of suitable activator such as H_2O_2 and the cleavage of DNA by the complex is dependent both on concentration of the complex and time of the

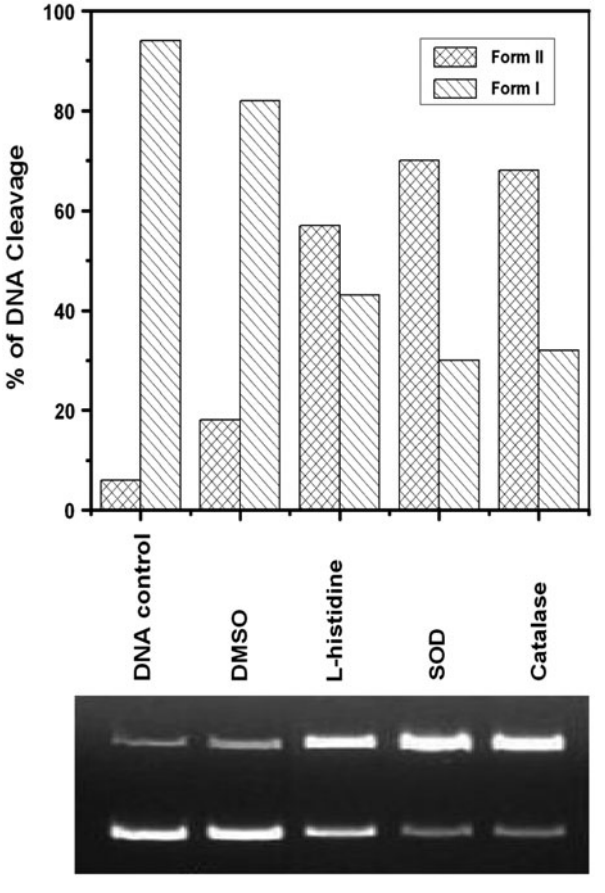

Figure 6. Influence of common radical scavengers on the cleavage of pUC19 plasmid DNA from Form I to Form II by **1** (60 μM) in the presence of H_2O_2 (100 μM) at 37 °C for the time span of 1 h.

reaction. The time dependent profile reveals that the disappearance of Form I and the appearance of Form II with reaction time show pseudo-first-order kinetic profiles and furnishes the pseudo-first-order rate constant of $4.16 \times 10^{-4}\,s^{-1}$ for **1**.

To understand the mechanism of nuclease activity, DNA cleavage was performed in the presence of hydroxyl radical scavenger (DMSO), singlet oxygen quencher (L-histidine), superoxide scavenger (superoxide dismutase enzyme SOD), and hydrogen peroxide scavenger (catalase) (figure 6). The results show that significant inhibition in DNA cleavage is observed in the presence of DMSO, suggesting that the freely diffusible hydroxyl radical is responsible for DNA cleavage exhibited by **1**. In a recent report, we have shown that mononuclear iron(II) and cobalt(III) complexes exhibit remarkable oxidative DNA cleavage activities in the presence of suitable activating agents(s) [34]. Only hydrogen peroxide was capable to interact with iron(II) for furnishing ROS, while both reducing and oxidizing agents were needed for initiating DNA cleavage by the cobalt(III) complex. The results suggest involvement of the cobalt(II) center is the key to generate such ROS for the nuclease activity. In the present heterobimetallic trinuclear **1**, the oxidation state of iron is + 3, and thus it is expected that iron(III) centers are not responsible for DNA cleavage. Like previous reports, the mechanism of DNA cleavage by **1** involves the wellknown Fenton type chemistry in which cobalt(II) of **1** reacts with hydrogen peroxide to generate the highly reactive hydroxyl radical.

Thus, the nuclease activity of **1** can be explained by the cooperation of two different metal sites present in the molecule, the aromatic rings in iron(III) centers are responsible for binding with DNA, while diffusible hydroxyl radical generated *in situ* by the reaction of cobalt(II) center with hydrogen peroxide is liable for cleavage of DNA. However, the chemical nuclease activity of **1** is significantly lower than that of similar cobalt(II) complexes [34, 57, 58], perhaps due to involvement of two different metals in DNA cleavage. As iron(III) sites interact with DNA in the groove region, the bent structure of **1** enforces the cobalt(II) center to hang away from DNA sugar moieties or nucleic bases, and thus shows lower DNA cleavage activity.

4. Conclusion

A cyanide-bridged heterobimetallic trinuclear complex **1** derived from the assembly of $(PPh_4)[Fe(pzcq)(CN)_3]$ with cobalt(II) nitrate is reported. Structural studies reveal that **1** is a bent complex in which each $[(pzcq)Fe(CN)_3]^-$ is a monodentate ligand through a cyanide to the central cobalt(II). The binding affinity of **1** to CT-DNA was examined by various techniques, and the results support groove binding of **1** to DNA. The nuclease activity in the presence of H_2O_2 showed that cleavage efficiency depends on the complex concentration and incubation period. Inhibition of nuclease activity was observed in the presence of radical scavengers and a possible role of diffusible hydroxyl radical is speculated. The DNA cleavage activity of **1** proceeds through cooperation of two different metal sites, the quinoline of pzcq in iron(III) centers are responsible for binding with DNA while diffusible hydroxyl radical seems to be involved in cleavage of DNA.

Supplementary material

Additional figures S1 and S2. CCDC 892467 contains the supplementary crystallographic data (without structure factors) for this paper. These data can be obtained free of charge via www.ccdc.cam.ac.uk/data_request/cif, by e-mailing data_request@ccdc.cam.ac.uk, or

by contacting the Cambridge Crystallographic Data Center, 12 Union Road, Cambridge CB2 IEZ, UK, Fax: +44(0)1223-336033; E-mail: deposit@ccdc.cam.ac.uk; website: http://www.ccdc.cam.ac.uk.

Acknowledgements

The author is thankful to the University Grant Commission (UGC), India (Sanction No. PSW-173/11-12) for financial support for this work. Instrumental facilities from Jadavpur University, India are also gratefully acknowledged.

References

[1] L.J.K. Boerner, J.M. Zaleski. *Curr. Opin. Chem. Biol.*, **9**, 135 (2005).
[2] T.A. Shell, D.L. Mohler. *Curr. Org. Chem.*, **11**, 1525 (2007).
[3] Q. Jiang, N. Xiao, P.F. Shi, Y.G. Zhu, Z.J. Guo. *Coord. Chem. Rev.*, **251**, 1951 (2007).
[4] K. Eisenschmidt, T. Lanio, A. Simoncsits, A. Jeltsch, V. Pingoud, W. Wende, A. Pingoud. *Nucleic Acids Res.*, **33**, 7039 (2005).
[5] M. Pitié, C. Boldron, G. Pratviel. *Adv. Inorg. Chem. Including Bioinorg. Stud.*, **58**, 77 (2006).
[6] M.J. Fernandez, B. Wilson, M. Palacios, M.M. Rodrigo, K.B. Grant, A. Lorente. *Bioconjugate Chem.*, **18**, 121 (2007).
[7] Y. Jin, J.A. Cowan. *J. Am. Chem. Soc.*, **127**, 8408 (2005).
[8] C.-L. Liu, M. Wang, T.-L. Zhang, H.-Z. Sun. *Coord. Chem. Rev.*, **248**, 147 (2004).
[9] E. Wong, C.M. Giandomenico. *Chem. Rev.*, **99**, 2451 (1999).
[10] L. Ronconi, P.J. Sadler. *Coord. Chem. Rev.*, **251**, 1633 (2007).
[11] J.M. Rademaker-Lakhai, D. Van den Bongard, D. Pluim, J.H. Beijnen, J.H. Schellens. *Clin. Cancer Res.*, **10**, 3717 (2004).
[12] A.C.G. Hotze, B.M. Kariuki, M.J. Hannon. *Angew. Chem. Int. Ed.*, **45**, 4839 (2006).
[13] P. Uma Maheswari, S. Roy, H.D. Dulk, S. Barends, G.V. Wezel, B. Kozlevcar, P. Gamez, J. Reedijk. *J. Am. Chem. Soc.*, **128**, 710 (2006).
[14] A. Barve, A. Kumbhar, M. Bhat, B. Joshi, R. Butcher, U. Sonawane, R. Joshi. *Inorg. Chem.*, **48**, 9120 (2009).
[15] B.C. Bales, T. Kodama, Y.N. Weledji, M. Pitie, B. Meunier, M.M. Greenberg. *Nucleic Acids Res.*, **33**, 5371 (2005).
[16] W. Szczepanik, J. Ciesiolka, J. Wrzesinski, J. Skala, M. Jezowska-Bojczuk. *Dalton Trans.*, 1488 (2003).
[17] X.L. Wang, H. Chao, H. Li, X.L. Hong, Y.J. Liu, L.F. Tan, L.N. Ji. *J. Inorg. Biochem.*, **98**, 1143 (2004).
[18] S. Ramakrishnan, E. Suresh, A. Riyasdeen, M.A. Akbarsha, M. Palaniandavar. *Dalton Trans.*, **40**, 3524 (2011).
[19] J. Widom, R.L. Baldwin. *Biopolymers*, **22**, 1595 (1983).
[20] R. Gust, I. Ott, D. Posselt, K. Sommer. *J. Med. Chem.*, **47**, 5837 (2004).
[21] C.C. Cheng, C.F. Luo, W.J. Wang. *Angew. Chem. Int. Ed. Engl.*, **38**, 1255 (1999).
[22] D. Lahiri, S. Roy, S. Saha, R. Majumdar, R.R. Dighe, A.R. Chakravarty. *Dalton Trans.*, **39**, 1807 (2010).
[23] D. Lahiri, T. Bhowmick, B. Pathak, O. Shameema, A.K. Patra, S. Ramakumar, A.R. Chakravarty. *Inorg. Chem.*, **48**, 339 (2009).
[24] J. Chen, J. Stubbe. *Curr. Opin. Chem. Biol.*, **8**, 175 (2004).
[25] W.K. Pogozelski, T.D. Tullius. *Chem. Rev.*, **98**, 1089 (1998).
[26] R.M. Burger. *Struct. Bond.*, **97**, 287 (2000).
[27] S.T. Hoehn, H.-D. Junker, R.C. Bunt, C.J. Turner, J. Stubbe. *Biochemistry*, **40**, 5894 (2001).
[28] M. Roy, S. Ramakumar, A.R. Chakravarty. *Dalton Trans.*, 1024 (2009).
[29] M. Valko, M. Izakovic, M. Mazur, C.J. Rhodes, J. Telser. *Mol. Cell. Biochem.*, **266**, 37 (2004).
[30] A.J. Danford, D. Wang, Q. Wang, T.D. Tullius, S.J. Lippard. *Proc. Nat. Acad. Sci. U.S.A.*, **102**, 12311 (2005).
[31] J. Yuan, D.B. Lovejoy, D.R. Richardson. *Blood*, **104**, 1450 (2004).
[32] D.R. Richardson, P.C. Sharpe, D.B. Lovejoy, D. Senaratne, D.S. Kalinowski, M. Islam, P.V. Bernhardt. *J. Med. Chem.*, **49**, 6510 (2006).
[33] A. Panja, T. Matsuo, S. Nagao, S. Hirota. *Inorg. Chem.*, **50**, 11437 (2011).
[34] A. Panja. *Polyhedron*, **43**, 22 (2012).
[35] J. Il Kim, H.S. Yoo, E.K. Koh, C.S. Hong. *Inorg. Chem.*, **46**, 8481 (2007).

[36] Z. Otwinowski, W. Minor. In *Methods in Enzymology*, C.W. Carter, Jr., R.M. Sweet (Eds.), pp. 307–326, Academic Press, New York, NY (1997), Vol. 276.
[37] G.M. Sheldrick. *SHELXL97, Program for Crystal Structure Refinement*, University of Göttingen, Göttingen (1997).
[38] L.J. Farrugia. *J. Appl. Crystallogr.*, **32**, 837 (1999).
[39] J. Marmur. *J. Mol. Biol.*, **3**, 208 (1961).
[40] M.E. Reichmann, S.A. Rice, C.A. Thomas, P. Doty. *J. Am. Chem. Soc.*, **76**, 3047 (1954).
[41] S. Satyanarayana, J.C. Dabrowiak, J.B. Chaires. *Biochemistry*, **32**, 2573 (1993).
[42] M. González-Álvarez, G. Alzuet, J. Borraś, B. Maciás, A. Castiñeiras. *Inorg. Chem.*, **42**, 2992 (2003).
[43] R. Lescouëzec, J. Vaissermann, L.M. Toma, R. Carrasco, F. Lloret, M. Julve. *Inorg. Chem.*, **43**, 2234 (2004).
[44] Z.-H. Ni, H.-Z. Kou, L.-F. Zhang, W.-W. Ni, Y.-B. Jiang, A.-L. Cui, J. Ribas, O. Sato. *Inorg. Chem.*, **44**, 9631 (2005).
[45] J.I. Kim, H.Y. Kwak, J.H. Yoon, D.W. Ryu, I.Y. You, N. Yang, B.K. Cho, J.-G. Park, H. Lee, C.S. Hong. *Inorg. Chem.*, **48**, 2956 (2009).
[46] J.-Z. Gua, L. Jiang, M.-Y. Tan, T.-B. Lu. *J. Mol. Struct.*, **890**, 24 (2008).
[47] M.S. Deshpande, A.A. Kumbhar, A.S. Kumbhar. *Inorg. Chem.*, **46**, 5450 (2007).
[48] M.T. Carter, M. Rodriguez, A.J. Bard. *J. Am. Chem. Soc.*, **111**, 8901 (1989).
[49] J.B. Lepecq, C. Paoletti. *J. Mol. Biol.*, **27**, 87 (1967).
[50] B.C. Baguley, M. Lebert. *Biochemistry*, **23**, 937 (1984).
[51] H. Wu, J. Yuan, Y. Bai, G. Pan, H. Wang, X. Shu, G. Yu. *J. Coord. Chem.*, **65**, 616 (2012).
[52] J.R. Lakowicz, G. Webber. *Biochemistry*, **12**, 4161 (1973).
[53] D.L. Boger, B.E. Fink, S.R. Brunette, W.C. Tse, M.P. Hedrick. *J. Am. Chem. Soc.*, **123**, 5878 (2001).
[54] G. Yang, J.Z. Wu, L. Wang, L.-N. Ji, X. Tian. *J. Inorg. Biochem.*, **66**, 141 (1997).
[55] L.N. Ji, X.H. Zou, J.G. Liu. *Coord. Chem. Rev.*, **216–217**, 513 (2001).
[56] Y.J. Liu, H. Chao, L.F. Tan, X.Y. Yuan, W. Wei, L.N. Ji. *J. Inorg. Biochem.*, **99**, 530 (2005).
[57] S. Ramakrishnan, E. Suresh, A. Riyasdeen, M.A. Akbarsha, M. Palaniandavar. *Dalton Trans.*, **40**, 3245 (2011).
[58] R. Indumathy, M. Kanthimathi, T. Weyhermuller, B.U. Nair. *Polyhedron*, **27**, 3443 (2008).